

MOL #43208

SMALL-MOLECULE SCREEN IDENTIFIES INHIBITORS OF A HUMAN INTESTINAL CALCIUM-ACTIVATED CHLORIDE CHANNEL

Ricardo De La Fuente, Wan Namkung*, Aaron Mills* and A. S. Verkman

Departments of Medicine and Physiology, Cardiovascular Research Institute,
University of California, San Francisco CA, 94143-0521, U.S.A.

MOL #43208

RUNNING TITLE PAGE

Running title: Small-molecule CaCC inhibitors

Corresponding author:

Alan S. Verkman, M.D., Ph.D.

1246 Health Sciences East Tower, Box 0521

University of California, San Francisco CA 94143-0521, U.S.A.

Phone: (415)-476-8530; Fax: (415)-665-3847

E-mail: Alan.Verkman@ucsf.edu; <http://www.ucsf.edu/verklab>

Number of text pages: 30

Number of tables: 2

Number of figures: 8

Number of references: 40

Number of words in Abstract: 182

Number of words in Introduction: 488

Number of words in Discussion: 602

List of abbreviations: CaCC, calcium-activated chloride channel; CaMKII, calcium-calmodulin kinase II; CFTR, cystic fibrosis transmembrane conductance regulator; YFP, yellow fluorescent protein

MOL #43208

ABSTRACT

Calcium-activated chloride channels (CaCCs) are widely expressed in mammalian tissues, including intestinal epithelia, where they facilitate fluid secretion. Potent, selective CaCC inhibitors have not been available. We established a high-throughput screen for identification of inhibitors of a human intestinal CaCC based on inhibition of ATP/carbachol-stimulated iodide influx in HT-29 cells after lentiviral infection with the fluorescent halide-sensing protein YFP-H148Q/I152L. Screening of 50,000 diverse, drug-like compounds yielded six classes of putative CaCC inhibitors, two of which, 3-acyl-2-aminothiophenes and 5-aryl-2-aminothiazoles, inhibited by >95% iodide influx in HT-29 cells in response to multiple calcium-elevating agonists, including thapsigargin, without inhibition of calcium elevation, CaMKII activation, or CFTR chloride channels. These compounds also inhibited calcium-dependent chloride secretion in T84 human intestinal epithelial cells. Patch-clamp analysis indicated inhibition of CaCC gating, which together with the calcium-calmodulin data, suggests that the inhibitors target the CaCC directly. Structure-activity relationships were established from analysis of more than 1800 analogs, with IC₅₀s of the best analogs down to ~1 μ M. Small-molecule CaCC inhibitors may be useful in pharmacological dissection of CaCC functions, and in reducing intestinal fluid losses in CaCC-mediated secretory diarrheas.

INTRODUCTION

There are at least five distinct classes of mammalian Cl⁻ channels, including the cystic fibrosis transmembrane conductance regulator (CFTR), CLC-type voltage-sensitive Cl⁻ channels, ligand-gated (GABA and glycine) Cl⁻ channels, volume-sensitive Cl⁻ channels, and calcium-activated Cl⁻ channels (CaCCs) (reviewed in Eggermont, 2004; Hartzell et al., 2005a). The molecular identities of epithelial cell CaCCs remain unclear, with potential candidates including *bestrophins* (Best1-Best4), CLCs of the *CKCA* family, and products of the recently described *tweety* gene (Hartzell et al., 2005b; Loewen and Forsyth, 2005; Suzuki, 2006). Evidence has been reported suggesting that CaCC(s) in intestinal epithelial cells provide an important route for Cl⁻ and fluid secretion in secretory diarrheas caused by certain drugs (antiretrovirals, chemotherapeutics) and viruses (Morris et al. 1999, Barrett, 2000; Kidd and Thorn, 2000; Takahashi et al. 2000; Gyomory et al. 2001; Rufo et al. 2004; Thiagarajah and Verkman, 2005; Schultheiss et al. 2005, 2006; Farthing, 2006; Lorrot and Vasseur, 2007). Smooth muscle CaCCs have been implicated in the pathophysiology of asthma (Bolton, 2006). Airway CaCCs are found in some model systems to be upregulated in cystic fibrosis (Tarran et al. 2002), providing an alternative chloride conductance to compensate for missing or defective CFTR.

A significant limitation in studying CaCCs has been the lack of potent or selective inhibitors. Available compounds, including fenamates, anthracene-9-carboxylic acid, indayloxyacetic acid, ethacrynic acid and tamoxifen have low potency and inhibit multiple types of Cl⁻ channels and transporters, and in some cases cause activation of BK_{Ca} K⁺ channels (Hartzell et al., 2005a). Small-molecule CaCC inhibitors are predicted to be of potential utility in the therapy of certain secretory diarrheas, and of excess mucus secretion in asthma and cystic fibrosis (Morris et al. 1999; Rufo et al. 2004; Barnes, 2005; Cuthbert, 2006; Hegab et al. 2007).

MOL #43208

The purpose of this study was to identify small-molecule inhibitors of a human intestinal CaCC that target the channel itself or site(s) distal to calcium elevation. Because the molecular identity of intestinal epithelial CaCC(s) is not known, we developed a phenotype-based screening assay using a human intestinal epithelial cell line (HT-29) that grew well after lentiviral expression of a yellow fluorescent protein (YFP)-type halide sensor (YFP-H148Q/I152L, Jayaraman et al. 2000). As diagrammed in Fig. 1A, the cell-based assay involved measurement of iodide influx in a monolayer of YFP-expressing HT-29 cells in response to a combination of calcium-elevating agonists. A combination of agonists was used to prevent or at least minimize the identification of compounds that target site(s) proximal to cell calcium elevation. CaCC function was quantified from iodide influx as measured from the kinetics of YFP fluorescence quenching following extracellular iodide addition. YFP-expressing epithelial cells have been used in our lab in similar screens to identify small-molecule activators and inhibitors of wildtype and mutant CFTRs (Ma et al., 2002ab; Yang et al. 2003; Muanprasat et al. 2004; Pedemonte et al. 2005). Compounds with apparent CaCC inhibition activity were prioritized, resynthesized, analyzed for mechanism-of-action, and subject to structure-activity analysis.

METHODS

Cell culture and infection

HT-29 cells (ATCC HTB-38) were obtained from the American Type Culture Collection and grown in DMEM supplemented with 10% fetal bovine serum (FBS), 100 units/ml penicillin and 100 µg/ml streptomycin. T84 cells (ATCC CCL-248) were maintained in DMEM/F12 (1:1) medium containing 10% FBS, 100 units/ml penicillin and 100 µg/ml streptomycin. Fisher rat thyroid (FRT) cells expressing human CFTR and YFP-H148Q/I152L were generated as described (Ma et al. 2002a), and grown in F-12 Modified Coon's medium

MOL #43208

supplemented with 10% FBS, 2 mM glutamine, 100 units/ml penicillin and 100 µg/ml streptomycin. All cells were grown at 37 °C in 5% CO₂ / 95% air.

For infection of HT-29 cells with lentivirus encoding YFP-H148Q/I152L, cells were cultured in 90-mm diameter plates in McCoy's 5a medium supplemented with 1.5 mM L-glutamine, 10% FBS and 2.2 g/L sodium bicarbonate. Cells were cultured until ~80% confluence. Cells were washed three times with PBS, and then 1 ml of a high-titer lentiviral supernatant was added to each well in the presence of 8 µg/ml polybrene. Cells were incubated at 37 °C in 5% CO₂ / 95% air for 6 hours and medium was then replaced with the regular DMEM growth medium described above. YFP expression was detected in >90% of cells 48 h after infection.

Compounds

Compounds for primary screening were purchased from ChemDiv (San Diego, CA). The compound collection contained 50,000 diverse, drug-like compounds with >90% of compounds in the molecular size range 200-450 daltons. Compounds for the secondary screening were purchased from ChemDiv and Asinex. Compounds were prepared in 96-well plates (Corning-Costar) as 10 mM solutions in dimethylsulfoxide (DMSO). For the primary screen compounds were tested in groups of 4 compounds per well.

Screening procedures

Screening was done using a customized screening system (Beckman Coulter, Inc., Indianapolis, IN) consisting of the SAGIAN Core system integrated with SAMI software, and equipped with an ORCA arm for labware transport, a 96-channel head Biomek FX, CO₂ incubator, plate washer, bar code reader, delidding station, and two FLUOstar Optima fluorescence plate readers (BMG Labtechnologies, Durham, North Carolina), each equipped with syringe pumps and custom excitation / emission filters (500 / 544 nm; Chroma, Brattleboro, VT). HT-29 cells

MOL #43208

expressing YFP-H148Q/I152L were plated in 96-well plates at 70% confluence. Plates were incubated overnight at 37 °C, 5% CO₂ and then the growth medium was replaced with fresh growth medium. Cells were incubated further until 95% confluence (12-18 h), washed 3 times with PBS, and incubated with the test compounds at 32.5 μM final concentration for 5 min in PBS, in a final volume of 60 μl/well. YFP fluorescence was measured for 1 s before and 30 s after addition of a PBS-iodide solution (PBS with 100 mM chloride replaced by iodide) containing carbachol and ATP (100 μM each). Each 96-well plate contained 'positive' controls (DMSO vehicle without agonists or test compounds) and 'negative' controls (DMSO vehicle with agonists but without test compounds). In some experiments solutions included (individually or in combination): carbachol, ATP or histamine (at 50, 100, 150 or 200 μM), calcimycin (10 μM), thapsigargin (2 μM) and CFTR_{inh}-172 (20 μM). All chemicals were purchased from Sigma-Aldrich. For experiments with thapsigargin or calcimycin, cells in 96-well plates at 100% confluence were washed 3 times with PBS, incubated with test compounds at 32.5 μM for 5 min in PBS in a final volume of 60 μl/well, and then incubated with 2 μM thapsigargin for 7 min or 10 μM calcimycin for 3 min before assay of iodide influx. Iodide influx (d[I⁻]/dt at t=0) was computed from fluorescence time course data by single exponential regression, as described (Ma et al. 2002a). Percentage inhibition was computed as: percentage inhibition = 100 x (Slope_{negative control} - Slope_{test compound}) / (Slope_{negative control} - Slope_{positive control}).

CFTR functional assay

As described (Ma et al. 2002a), FRT cells expressing human wildtype CFTR and YFP-H148Q/I152L, at 100% confluence, were washed 3 times with PBS, leaving 60 μL. CFTR was activated by a cocktail containing forskolin (20 μM), genistein (50 μM) and isobutylmethylxanthine (100 μM). Iodide influx was measured at 10 min after addition of test compounds by following YFP fluorescence for 2 s before and 20 s after addition of 165 μl of PBS-iodide.

MOL #43208

Synthesis procedures

CaCC_{inh}-A01: For synthesis of 6-*t*-butyl-2-(furan-2-carboxamido)-4,5,6,7-tetrahydrobenzo[*b*] thiophene-3-carboxylic acid **1**, a mixture of 4-(*t*-butyl) cyclohexanone (0.154 g, 1.00 mmol), methyl-2-cyanoacetate (0.109 g, 1.1 mmol), morpholine (0.104 g, 1.2 mmol) and elemental sulfur (0.048 g, 1.5 mmol) in methanol (5 mL) were reacted for 10 min at 120 °C using a Biotage microwave reactor. Purification by flash chromatography afforded **1** (0.242 g, 0.91 mmol) in 91% yield (Gewald and Hofmann, 1969; Srinidhar et al. 2007). Acylation of the amine with furfuryl chloride (0.186 mg, 0.70 mmol) gave compound **2** in 87% yield. Ester hydrolysis of **2** (0.179 g, 0.500 mmol) was accomplished with NaOH in methanol, giving *t*-butylbenzothiophene **3** (CaCC_{inh}-A1). CaCC_{inh}-A01 was purified by column chromatography (160 mg, 93 % yield). ¹H NMR (400 MHz, CDCl₃): □ 12.88 (s, 1H), 7.59 (s, 1H), 7.30 (d, J = 3.2 Hz, 1H), 6.59 (dd, J = 7.6 Hz and 2.0 Hz, 1H), 3.18 (d, 2H), 2.72 (m, 2H), 2.43 (t, 1H), 2.05 (m, 1H), 1.51 (m, 1H), 1.35 (m, 1H), 0.95 (s, 9H); ¹³C NMR (CDCl₃): □ 179.2, 170.6, 154.8, 149.1, 146.8, 145.4, 131.8, 128.3, 116.6, 112.9, 94.5, 45.1, 32.6, 27.4, 26.0, 24.5; LC-MS: m/z 346.16 [M+ H]⁺ (Nova-Pak C₁₈ column, 99%, 200-400 nm).

CaCC_{inh}-B01: The synthesis of 2-hydroxy-4-(4-*p*-tolylthiazol-2-ylaminobenzoic acid **4** began with the synthesis of thiourea **5**. Reaction of thiophosgene (2.7 g, 23.890 mmol) with 4-amino-2-hydroxybenzoic acid **2** (3.06 g, 20 mol) in aqueous HCl (41 mL) gave thioisocyanate **4** by crystallization in 83% yield (Seligman et al. 1953). Treatment of thioisocyanate **4** with ammonium hydroxide gave thiourea **5** in 84% yield. Thiazole cyclization of thiourea **5** (0.300 g, 1.415 mmol) with 2-bromo-1-*p*-tolylethanone (0.298 g, 1.415 mmol) in EtOH (15 mL) gave aminothiazole **6**. The aminothiazole was purified by column chromatography to give CaCC_{inh}-B01 (406 mg, 88% yield). ¹H NMR (400 MHz, CDCl₃): □ 10.67 (s, 1H), 7.80 (d, J = 8.0 Hz, 2H), 7.71 (d, J = 8.1 Hz, 1H), 7.58 (d, J = 2.0 Hz, 1H), 7.36 (s, 1H), 7.25 (d, J = 8.0, 2H), 7.04 (dd, J = 8.1 Hz and 2.0 Hz,

MOL #43208

1H), 2.49 (s, 1H), 2.31 (s, 3H); ^{13}C NMR (CDCl_3): \square 171.7, 162.7, 162.0, 150.3, 147.2, 137.2, 131.7, 131.3, 129.3, 125.6, 108.5, 105.4, 103.6, 103.1, 20.8; LC-MS: m/z 327.11 $[\text{M} + \text{H}]^+$ (Nova-Pak C_{18} column, 97%, 200-400 nm).

Short-circuit current measurements

T84 cells were seeded at a density of 10^5 cells/cm² on permeable supports (Snapwell, 1.12 cm² surface area) and grown until confluent. Supports containing confluent cell monolayers were mounted in Snapwell inserts. Cells were bathed for a 30 min stabilization period in HCO_3^- -buffered solution containing (mmol/L): 120 NaCl, 5 KCl, 1 MgCl_2 , 1 CaCl_2 , 10 D-glucose, 5 HEPES and 25 NaHCO_3 (pH 7.4), aerated with 95% O_2 / 5% CO_2 at 37 °C. Monolayers were voltage-clamped at 0 mV (EVC4000 Multi-Channel V/I Clamp, World Precision Instruments), and short-circuit current (I_{sc}) was recorded continuously with agonists/inhibitors added at specified times.

Patch-clamp

Whole cell recordings were done on HT-29 cells at room temperature. The pipette solution contained (in mM): 30 CsCl, 100 Cs-aspartate, 1 MgCl_2 , 0.5 EGTA, 2 Tris-ATP, and 10 HEPES (pH 7.2 with CsOH), and the bath solution contained 140 N-methyl-D-glucamine chloride (NMDG-Cl), 1 CaCl_2 , 1 MgCl_2 , 10 glucose, and 10 HEPES (pH 7.2). In one set of studies symmetric NMDG-Cl solutions contained (in mM): 140 NMDG-Cl, 1 MgCl_2 , 0.5 EGTA, 2 Tris-ATP, and 10 HEPES (pH 7.2). Pipettes were pulled from borosilicate glass and had resistances of 3–5 $\text{M}\Omega$ after fire polishing. Seal resistances were typically between 3 to 10 $\text{G}\Omega$. After establishing the whole cell configuration, CaCCs were activated by 1 μM ionomycin. Whole-cell currents were elicited by applying hyperpolarizing and depolarizing voltage pulses from a holding potential of 0 mV to potentials between -120 mV and +120 mV in steps of 20 mV. Currents were

MOL #43208

filtered at 5 kHz, and digitized and analyzed using an AxoScope 10.0 system with Digidata 1440A converter. Mean currents were expressed as current densities (pA/pF).

[Ca²⁺]_i measurements

[Ca²⁺]_i was measured in confluent monolayers of HT-29 cells after loading with Fura-2 (2 μM Fura-2-AM, 30 min, 37 °C). Labeled cells were mounted in a perfusion chamber on the stage of an inverted epifluorescence microscope. Cells were superfused with (in mM): 140 NaCl, 5 KCl, 1 MgCl₂, 1 CaCl₂, 10 D-glucose, and 10 HEPES (pH 7.4), initially without and then with ATP / carbachol. Test compounds were present in some experiments for 10 min prior to agonist addition. Fura-2 fluorescence was recorded at excitation wavelengths of 340 nm and 380 nm using standard procedures.

Immunoblotting

Calcium/calmodulin-dependent protein kinase II (CaMKII) was activated by 2 min treatment of HT-29 cells with ATP / carbachol (each 100 μM). Cells were then lysed with cell lysis buffer (20 mM Tris-HCl (pH 7.4), 1% Triton X-100, 150 mM NaCl, 2 mM EDTA, 50 mM α-glycerolphosphate, 1 mM Na₃VO₄, 1 mM DTT, and protease inhibitor mixture (Roche Applied Science)). Cell debris was removed by centrifugation, and proteins in the supernatant were resolved by SDS-PAGE and immunoblotted using standard procedures (transfer to PDVF membrane, 1 h blocking in 5% nonfat dry milk, primary/secondary antibody incubations, enhanced chemiluminescence detection). Rabbit polyclonal antibodies for anti-phospho-CaMKII (Thr286) and β-actin were purchased from Cell Signaling Technology (Danvers, MA).

MOL #43208

RESULTS

High-throughput screening assay development and validation

As diagrammed in Fig. 1A, our assay utilized a human intestinal cell line (HT-29) having robust CaCC activity. In the presence of calcium-elevating agonist(s), extracellular iodide addition results in CaCC-facilitated iodide influx, which is detected by fluorescence quenching of a cytoplasmic YFP-based halide sensor (YFP-H148Q/I152L). After lentiviral infection, HT-29 cells stably expressing YFP-H148Q/I152L were brightly fluorescent, with nearly all cells showing fluorescence (Fig. 1B). Alternative human intestinal epithelial cells lines, including T84 and Caco-2 cells, were found to be inadequate for screening because of slow growth, lack of growth to confluent monolayers, poor YFP expression, and/or weak CaCC activity.

Several CaCC agonists were assayed to establish the cellular model for CaCC inhibitor screening. Histamine (100 μ M), calcimycin (10 μ M), ATP (100 μ M), carbachol (100 μ M) and forskolin (10 μ M) were tested individually (Fig. 2A) and in combinations (Fig. 2B). The CFTR inhibitor CFTR_{inh}-172 (20 μ M) was also tested. Of the agonists tested individually, carbachol and ATP produced the strongest responses as seen from the slopes of the fluorescence decrease following extracellular iodide addition. In combination, carbachol and ATP produced as large a response as seen for any of the combinations. Increased iodide influx was not found following forskolin addition, nor did CFTR_{inh}-172 inhibit iodide influx in response to calcium agonists, indicating that the cell clone used in our assay expressed little or no functional CFTR.

A combination of carbachol and ATP, each at high concentration, was selected for compound screening, reasoning that any inhibitors should act beyond the receptor binding step. Iodide influx measurements were done to establish agonist concentrations and addition times. Concentration dependence studies for carbachol (Fig. 2C) and ATP (not shown) indicated maximal responses at 100 μ M. Fig. 2D shows reduced iodide influx as a function of time between addition of 100 μ M carbachol / ATP and extracellular iodide, which is consequence of the transient

MOL #43208

elevation in cytoplasmic calcium produced by these agonists. The greatest iodide influx was found when agonists were added at ~10 s prior to iodide, though the influx was not much greater than when agonists were added at the time of iodide addition. For high-throughput screening, to simplify assay conditions, agonists (carbachol and ATP, each 100 μ M) were added together with iodide.

CaCC inhibitor identification by high-throughput screening

To characterize the assay as used for high-throughput screening, iodide influx was measured in the YFP-expressing HT-29 cells in a 96-well format using an automated workstation capable of assaying more than 10,000 compounds overnight. Fig. 3A (left) shows representative YFP fluorescence kinetics measured in single wells of 96-well plates. Each curve consisted of recording of baseline fluorescence for 1 second, followed by 30 seconds of continuous recording of fluorescence after rapid addition of a solution containing iodide and the CaCC agonist combination (carbachol and ATP, each 100 μ M). Following a small solution addition artifact, there was little decrease in fluorescence in the absence of activators, compared to a robust reduction in fluorescence with agonists. Fig. 3A (right) shows frequency histograms of iodide influx rates, $d[I]/dt$, in individual wells for ‘positive’ (no agonists, equivalent to 100% inhibition) and ‘negative’ (with agonists, 0% inhibition) controls. The computed Z' -factor (Verkman, 2004) for the assay was very good, 0.74, indicating adequacy of a single compound screening to identify putative CaCC inhibitors. The presence of DMSO (from compound addition) did not affect assay quality.

Based on initial small-scale screenings at different compound concentrations, which showed a low ‘hit’ rate for discovery of active compounds, we screened 50,000 compounds at a concentration 32.5 μ M. Fig. 3B (left) shows examples of data from single wells for compounds with ‘strong’, ‘weak’ and no inhibition activity. Fig. 3B (right) summarizes percentage inhibition data as a frequency histogram. Of 50,000 small molecules screened (in groups of four), 300

MOL #43208

compound groups had CaCC inhibitory activity as defined arbitrarily by a 70% cutoff (vertical dashed line). Retesting of these 300 compound groups indicated a false-positive rate of ~40%.

Further analysis was done on fifteen compound groups that produced greatest inhibition when retested at 10 and 30 μ M concentrations. The compound responsible for activity in each group was determined by testing of individual compounds. In each case a single active compound was identified in the groups of four. Fig. 4A shows structures of the most active of six classes of putative CaCC inhibitors (classes A-F) identified by single compound testing; in some cases, particularly for classes A and B, similar structures were seen several times. These structures are unrelated to all known Cl⁻ channel inhibitors. Percentage inhibition of these compounds at 30 μ M was in the range 60 to >90 %. Based on multiple criteria, including potency, water solubility, drug-like properties, identification of active analogs, chemical stability and CaCC targeting, we focused attention on compounds of classes A and B. As shown below, the class E compound did not inhibit iodide influx in response to thapsigargin, suggesting that its target is proximal in the calcium signaling pathway, and thus not of interest here. The class D compound was determined to have poor stability in aqueous solutions, likely because of retro-Diels-Alder reaction. Class F compounds were excluded from further study because of their small size and relatively low potency.

Synthesis and characterization of class A and B compounds

Prior to further analysis of their biological activities and mechanisms-of-action, we synthesized the class A and B compounds to high purity and verified their structures and chemical stability in aqueous solutions. The synthesis of CaCC_{inh}-A01 was accomplished in three steps (Fig. 4B, top), involving Knoevenagel condensation of methyl cyanoacetate with t-butylcyclohexanone followed by cyclization on elemental sulfur. Purification by flash chromatography produced the 2-aminothiophene Gewald product. Acyclation of the aminothiophene gave the N-acyl methyl ester **2**

MOL #43208

in good yield. Ester **2** was hydrolyzed with NaOH to give CaCC_{inh}-A01 **3**, which was purified by chromatography and recrystallization. Synthesis of CaCC_{inh}-B01 also involved three steps (Fig. 4B, bottom). Reaction of 4-amino-2-hydroxybenzoic acid with thiophosgene in HCl gave isothiocyanate **4** in good yield. Treatment of **4** with ammonium hydroxide gave thiourea **5**, which was then reacted with 2-bromo-1-p-tolyethanone to give CaCC_{inh}-B01 **6**.

CaCC_{inh}-A01 and CaCC_{inh}-B01 were confirmed by ¹H-NMR, ¹³C-NMR and mass spectrometry (analytical data provided in Methods). The aqueous solubility of CaCC_{inh}-A01 and CaCC_{inh}-B01 in PBS was >500 μM, as measured by optical absorbance of a saturated solution after appropriate dilution. The high aqueous solubility of CaCC_{inh}-A01 and CaCC_{inh}-B01 is a consequence of their polarity and negative charge at physiological pH. By liquid chromatography purity was >97% and 99% for CaCC_{inh}-A01 and CaCC_{inh}-B01, respectively.

Testing of the purified compounds using the fluorescence plater reader assay verified their activities, with IC₅₀ values ~10 μM (Fig. 4C). These apparent IC₅₀ values are only semi-quantitative because of the multi-step nature of the screening assay and because of the ~3-fold compound dilution at the time of iodide addition during the assay. Accurate IC₅₀s were determined by electrophysiological assays (see below).

Target identification

Several targets are possible based on the screening strategy in Fig. 1A, including ligand-receptor binding, calcium elevation, calcium-calmodulin (CaMKII) signaling and the CaCC itself. To distinguish between pre- and post-calcium signaling targets, compounds of each class were tested following stimulation of HT-29 cells by thapsigargin, which produces calcium elevation without ligand-receptor binding or phosphoinositide signaling. Fig. 5A shows that each of the compounds inhibited iodide influx following thapsigargin, except for the class E compound, whose target is thus likely upstream of calcium signaling. Experiments were also done to rule out

MOL #43208

compound effects on CFTR, as CFTR is a major intestinal chloride channel and there is evidence for cross-talk between cAMP and calcium signaling in intestinal cell chloride secretion (Chao et al. 1994; Takahashi et al. 2000; Schultheiss et al. 2006). Using our well-established FRT-CFTR assay, Fig. 5B shows no CFTR inhibition by any of the compounds at 30 μM , with CFTR_{inh}-172 inhibition shown as positive control.

Measurements of cytoplasmic calcium were done to investigate whether CaCC_{inh}-A01 and CaCC_{inh}-B01 interfered with agonist-induced calcium signaling in HT-29 cells. Fig. 5C shows $[\text{Ca}^{2+}]_i$ elevations in response to 1 μM ATP, 100 μM ATP and 100 μM carbachol (left), or 1 μM ionomycin (middle). Pretreatment with CaCC_{inh}-A01 or CaCC_{inh}-B01 at high concentration prior to agonist addition did not significantly reduce the ATP- or carbachol-induced $[\text{Ca}^{2+}]_i$ elevations (right).

Regulation of CaCC activation by CaMKII occurs in a cell type-dependent manner (Hartzell et al., 2005a). CaMKII has been reported to regulate calcium-activated chloride currents in HT-29 and T84 cells (Worrell and Frizzell, 1991; Morris and Frizzell, 1993; Chan et al. 1994; Braunn and Schulman, 1995). To determine whether the CaCC inhibitors interfered with ATP / carbachol-induced CaMKII activation, CaMKII phosphorylation in HT-29 cells was measured by immunoblot analysis. CaMKII was activated by a 2 min incubation with 100 μM ATP / carbachol. Fig. 5D shows strong pCaMKII immunoreactivity following agonist treatment. Pretreatment with 30 μM CaCC_{inh}-A01 or CaCC_{inh}-B01 did not significantly affect agonist-induced CaMKII phosphorylation. β -actin is shown as a loading control.

Whole-cell patch-clamp was done to investigate the inhibition of calcium-dependent chloride current in HT-29 cells by CaCC_{inh}-A01 and CaCC_{inh}-B01. Measurements were carried out under K^+ -free conditions (Cs^+ in pipette) to ensure that chloride currents were being measured. Treatment with 1 μM ionomycin produced large currents of 28 ± 3 pA/pF ($V_m +100$ mV) in NMDG-Cl solutions, with an outwardly rectifying I-V relationship (Figs. 6A and B). Ionomycin-stimulated

MOL #43208

currents were measured when the current was maximally activated at a V_m of -40 mV and current density data was analyzed at V_m of +100 mV. As summarized in Fig. 6C, calcium-dependent chloride current was reduced by $38 \pm 14 \%$, $66 \pm 10 \%$, and $91 \pm 1 \%$ by 0.1, 1 and 10 μM CaCC_{inh}-A01, respectively, and by $11 \pm 7 \%$, $34 \pm 12 \%$, and $77 \pm 4 \%$ by 0.1, 1 and 10 μM CaCC_{inh}-B01. As a control to exclude interference by TRP and non-selective cation channels, ionomycin-induced chloride currents were also recorded in the whole-cell configuration using symmetric NMDG-Cl solutions (Fig. 6D). As predicted, pretreatment with CaCC_{inh}-A01 and CaCC_{inh}-B01 reduced ionomycin-induced currents.

Chloride secretion was also measured in T84 cells to investigate whether the CaCC inhibitors identified from screening of HT-29 cells also inhibit the CaCC in a different human intestinal cell line. ATP / carbachol were used to induce calcium-dependent chloride secretion in well-differentiated T84 cell monolayers. The increase in short-circuit current in response to carbachol (without inhibitors added) was similar in all experiments (Fig. 7A). Subsequent application of 100 μM ATP ~30 min later produced a large response (top curve), which was reduced in the presence of inhibitors (lower four curves). Carbachol and ATP-induced short-circuit currents are summarized in Fig. 7B. ATP-induced short-circuit currents were reduced by $38 \pm 7 \%$ and $78 \pm 3 \%$ at 10 and 30 μM CaCC_{inh}-A01, respectively, and by $29 \pm 11 \%$ and $64 \pm 3 \%$ by 10 and 30 μM CaCC_{inh}-B01.

Structure-activity analysis

An important characteristic of small molecules for drug development is the existence of many active chemical analogs ('evolvable' SAR) in order to allow optimization of drug properties. SAR analysis was performed on 936 commercially available aminothiophenes (class A analogs) and 944 aminothazoles (class B analogs). Tables 1 and 2 provide semi-quantitative CaCC inhibition data (from plate reader assay) for 18 active aminothiophenes (class A) and 14 active aminothiazoles (class B). Fig. 8 summarizes the SAR analysis in terms of the functional groups

MOL #43208

conferring CaCC inhibition activity based on consideration of data for all analogs tested. An essential moiety for strong activity in both compound classes was the presence of a carboxylic acid functional group, as has been found in most chloride channel inhibitors.

For class A compounds, *t*-butyl at position R₁ conferred the greatest inhibition; inhibition was reduced or lost when R₁ was methyl or H, as with analogs CaCC_{inh}-A12-A15 (many inactive methyl analogs not included in Table). Modification of the cyclohexyl ring system to cyclopentyl and cycloheptyl (varying *n*) indicated greatest activity with six membered rings. Several cycloheptylthiophenes were found to be active but much less potent than the six membered ring analogs. At R₂, hydroxy, methoxy, ethoxy and substituted phenyl amides were tolerated. If R₂ is OH, as in the carboxylic acid, then R₃ can be a substituted phenyl ring or heterocycle as seen in CaCC_{inh}-01-A05, -A15 and -A17. Methyl and ethyl esters were tolerated at R₂ if an alkyl carboxylic acid was present at R₃ as seen in CaCC_{inh}-A06-A11. Substituted phenyl amides at R₂ had weak activity as seen in CaCC_{inh}-A16 and CaCC_{inh}-A18. For R₃, activity was found for substituted phenyl rings, heterocycles, and alkyl carboxylic acids such as 3-carboxypropanamido, *trans*-3-carboxyacrylamido, and 2-carboxycyclohexane-carboxamido, but only when R₂ was OMe, OEt, or NHPH. Of the alkyl substituted carboxylic acids at R₃, the most active analog was the *trans*-3-carboxyacrylamido in CaCC_{inh}-A07. CO-phenyl substitutions at R₃ were tolerated in active compounds with the 2-position favored. Electron-donating substituents led to substantially reduced activity. A variety of heterocycles were screened at R₃ with only CO-furfuryl active. The most potent compound was 6-*tert*-butyl-2-(cyclopenta-1,3-dienecarboxamido)-4,5,6,7-tetrahydrobenzo[*b*]thiophene-3-carboxylic acid (CaCC_{inh}-A01).

For class B, at position R₁ methyl substitution at the 4 position of the aromatic ring was present in most active compounds as seen in CaCC_{inh}-B01-B06. Additional methyl substitution at the 2 position gave active analogs CaCC_{inh}-B07-B09. Inhibition was greatly reduced when the phenyl ring was substituted at the 2 or 3 positions. As with Class A, a carboxylic acid functional

MOL #43208

group was essential for activity, either with an alkyl substitution at R₂ or a phenyl substitution at R₃. Loss of this carboxylic acid functionality reduced activity as seen in CaCC_{inh}-B09-B13. At position R₂ most active compounds contained either hydrogen substitution or an acetic acid group. For position R₃, a variety of phenyl substitutions were tolerated, the majority being alkyl or halogen substitution at the 3 and 4 positions. Electron donating substituents produced inactive compounds. The SAR study thus indicates the existence of many active class A and class B CaCC inhibitors having a wide range of potencies.

DISCUSSION

Our phenotype-based small-molecule screen identified novel chemical classes of inhibitors of CaCC conductance, two of which appear to target the CaCC itself rather than upstream signaling mechanisms. The aminothiophenes and aminothazoles did not interfere with agonist-induced cytoplasmic calcium elevation or calmodulin (CaMKII) phosphorylation, and by patch-clamp analysis inhibited CaCC gating. The data here do not distinguish between an external vs. internal site of compound action, nor do they provide information about the molecular identity of the intestinal CaCC responsible for the observed chloride conductance, though determination of comparative compound potencies on candidate CaCCs, as mentioned in the Introduction, may offer indirect evidence about CaCC identity. The verified 'hit' rate for our small-molecule screen, ~1 per 10,000 compounds tested, is in the range generally found in ion channel inhibitor screens. Therefore, further screening of larger collections of diverse compounds is likely to succeed in identifying new chemical classes of CaCCs.

Our high-throughput screening assay utilized a kinetic fluorescence measurement of iodide influx in an intestinal epithelial cell line. Iodide is superior to chloride for primary screening because of its transport by channels and not by exchangers or cotransporters, such as AE1 (Cl⁻/HCO₃⁻) and NKCC (Na⁺/K⁺/2Cl⁻), and its substantially greater quenching compared to chloride of

MOL #43208

available molecular and chemical halide sensors (Verkman and Jayaraman, 2002). Further, of specific relevance to the CaCC screening here, all CaCCs that have been tested show greater iodide vs. chloride conductance (Eggermont, 2004; Hartzell et al. 2005). The YFP indicator used for screening, YFP-H148Q/I152L, which is 50% quenched by ~3 mM iodide, was discovered by screening of ~1000 YFP analogs for halide sensitivity (Galiotta et al. 2001). YFPs have been applied, in other cell types, for small-molecule screens to identify inhibitors (Ma et al. 2002b; Muanprasat et al. 2004) and activators (Ma et al. 2002a) of wildtype CFTR, and for potentiators (Yang et al. 2003) and correctors (Pedemonte et al. 2005) of $\Delta F508$ -CFTR, the major CFTR mutation causing cystic fibrosis. We have also used a YFP/iodide screening strategy in a 'pathway' screen to identify G-protein coupled receptor antagonists (Yangthara et al. 2007). The cell line used here and the introduction method for stable YFP expression were selected after screening of existing human intestinal epithelial cell lines (T84, HT-29, Caco-2) and transfection methods (plasmids, viruses). Lentiviral introduction of YFP in HT-29 cells produced a cell line suitable for screening that fulfilled the key requirements of efficient growth on plastic, bright YFP fluorescence, strong CaCC chloride conductance, and low basal (CaCC-independent) iodide conductance.

CaCC(s) have been reported previously to be expressed in undifferentiated HT-29 and T84 cells (Morris and Frizzell, 1991; Worrell and Frizzell, 1991; Chan et al. 1994; Arreola et al. 1995; Braun and Schulman, 1995). Our patch-clamp and short-circuit current results are in agreement with these prior data. We found ionomycin-induced calcium-dependent chloride currents in HT-29 cells with typical outwardly-rectifying current-voltage relationships (Arreola et al. 1995; Braun and Schulman, 1995; Nilius et al. 1997), as well as ionomycin-induced calcium-dependent chloride current in T84 cells. Chloride currents in both cell types were strongly inhibited by the aminothiophenes and aminothazoles discovered here, suggesting common CaCC(s) in these cell types and indicating little or no inhibitor-insensitive calcium-dependent chloride current.

In summary, we report the development and validation of an efficient screen for

MOL #43208

identification of inhibitors of intestinal CaCCs, along with the identification and characterization of several classes of active compounds identified in a screen of 50,000 compounds. These or other compounds identified from similar screens, with follow-on work, may be useful for molecular identification of CaCCs and for therapeutic applications in certain secretory diarrheas and in lung diseases associated with mucus overproduction.

MOL #43208

References

- Arreola J, Melvin JE, and Begenisich T (1995) Inhibition of Ca^{2+} -dependent Cl^- channels from secretory epithelial cells by low internal pH. *J Membr Biol* **147**:95-104
- Barnes PJ (2005) Emerging targets for COPD therapy. *Curr Drug Targets Inflamm Allergy* **4**:675-683
- Barrett KE, Keely SJ (2000) Chloride secretion by the intestinal epithelium: molecular basis and regulatory aspects. *Annu Rev Physiol* **62**:535-572
- Bolton TB (2006) Calcium events in smooth muscles and their interstitial cells; physiological roles of sparks. *J Physiol* **570**:5-11
- Braun AP, Schulman H (1995) A non-selective cation current activated via the multifunctional Ca^{2+} -calmodulin-dependent protein kinase in human epithelial cells. *J Physiol* **488**:37-55
- Chan HC, Kaetzel MA, Gotter AL, Dedman JR, and Nelson DJ (1994) Annexin IV inhibits calmodulin-dependent protein kinase II-activated chloride conductance A novel mechanism for ion channel regulation. *J Biol Chem* **269**:32464-32468
- Chao AC, de Sauvage FJ, Dong YJ, Wagner JA, Goeddel DV, and Gardner P (1994) Activation of intestinal CFTR Cl^- channel by heat-stable enterotoxin and guanylin via cAMP-dependent protein kinase. *EMBO J* **13**:1065-1072
- Cuthbert AW (2006) The prospects of pharmacotherapy for cystic fibrosis. *J R Soc Med* **99**:30-35
- Eggermont J (2004) Calcium-activated chloride channels: (un)known, (un)loved? *Proc Am Thorac Soc* **1**:22-27

MOL #43208

Farthing MJ (2006) Antisecretory drugs for diarrheal disease. *Dig Dis* **24**, 47-58

Galiotta LJV, Haggie PM, and Verkman AS (2001) Green fluorescent protein-based halide indicators with improved chloride and iodide affinities. *FEBS Lett* **499**:220-224

Gewald K, and Hofmann I (1969) Heterocycles from CH-acid nitriles XV Reaction of ketones with cyanoacetic acid hydrazide and sulfur. *J Prakt Chem* **311**:402-407

Gyömörey K, Garami E, Galley K, Rommens JM, and Bear CE (2001) Non-CFTR chloride channels likely contribute to secretion in the murine small intestine. *Pflugers Arch* **443 Suppl 1**, S103-S106

Hartzell C, Qu Z, Putzier I, Artinian L, Chien LT, and Cui Y (2005b) Looking chloride channels straight in the eye: bestrophins, lipofuscinosis and retinal degeneration. *Physiol (Bethesda)* **20**:292-302

Hartzell, C, Putzier, I, and Arreola, J (2005a) Calcium-activated chloride channels. *Annu Rev Physiol* **67**:719-758

Hegab AE, Sakamoto T, Nomura A, Ishii Y, Morishima Y, Iizuka T, Kiwamoto T, Matsuno Y, Homma S, and Sekizawa K (2007) Niflumic acid and AG-1478 reduce cigarette smoke-induced mucin synthesis: the role of hCLCA1. *Chest* **131**:1149-1156

Jayaraman S, Haggie P, Wachter R, Remington SJ, and Verkman AS (2000) Mechanism and cellular applications of a green fluorescent protein-based halide sensor. *J Biol Chem* **275**:6047-6050

Kidd JF, and Thorn P (2000) Intracellular Ca²⁺ and Cl⁻ channel activation in secretory cells. *Annu Rev Physiol* **62**:493-513

Loewen ME, and Forsyth GW (2005) Structure and function of CLCA proteins. *Physiol Rev* **85**:1061-1092

MOL #43208

Lorrot M, and Vasseur M (2007) How do the rotavirus NSP4 and bacterial enterotoxins lead differently to diarrhea? *Virology* **4**:31

Ma T, Thiagarajah JR, Yang H, Sonawane ND, Folli C, Galiotta LJ, and Verkman AS (2002a) Thiazolidinone CFTR inhibitor identified by high-throughput screening blocks cholera toxin-induced intestinal fluid secretion. *J Clin Invest* **110**, 1651-1658

Ma T, Vetrivel L, Yang H, Pedemonte N, Zegarra-Moran N, Galiotta LJ, and Verkman AS (2002b) High-affinity activators of CFTR chloride conductance identified by high-throughput screening. *J Biol Chem* **277**:37235-37241

Morris AP and Frizzell RA (1993) Ca²⁺-dependent Cl⁻ channels in undifferentiated human colonic cells (HT-29) II Regulation and rundown. *Am J Physiol* **264**:C977-C985

Morris AP, Scott JK, Ball JM, Zeng CQ, O'Neal WK, and Estes MK (1999) NSP4 elicits age-dependent diarrhea and Ca²⁺ mediated I⁻ influx into intestinal crypts of CF mice. *Am J Physiol* **277**:G431-G544

Muanprasat C, Sonawane ND, Salinas D, Taddei A, Galiotta LJ, and Verkman AS (2004) Discovery of glycine hydrazide pore-occluding CFTR inhibitors: mechanism, structure-activity analysis, and in vivo efficacy. *J Gen Physiol* **124**:125-137

Nilius B, Prenen J, Szucs G, Wei L, Tanzi F, Voets T, and Droogmans G (1997) Calcium-activated chloride channels in bovine pulmonary artery endothelial cells. *J Physiol* **498**:381-386

Pedemonte N, Lukacs GL, Du K, Zegarra-Moran O, Galiotta LJ, and Verkman AS (2005) Small molecule correctors of defective $\Delta F508$ -CFTR cellular processing identified by high-throughput screening. *J Clin Invest* **115**:2564-2571

MOL #43208

Rufo PA, Lin PW, Andrade A, Jiang L, Rameh L, Flexner C, Alper SL, and Lencer WI (2004) Diarrhea-associated HIV-1 APIs potentiate muscarinic activation of Cl⁻ secretion by T84 cells via prolongation of cytosolic Ca²⁺ signaling. *Am J Physiol* **264**:C998-C1008

Schultheiss G, Hennig B, Schunack W, Prinz G, and Diener M (2006) Histamine-induced ion secretion across rat distal colon: involvement of histamine H1 and H2 receptors. *Eur J Pharmacol* **546**:161-170

Schultheiss G, Siefjediers A, and Diener M (2005) Muscarinic receptor stimulation activates a Ca²⁺-dependent Cl⁻ conductance in rat distal colon. *J Membr Biol* **204**:117-127

Seligman RB, Bost RW, and McKee RL (1953) Derivatives of p-aminosalicylic acid. *J Am Chem Soc* **75**:6334-6335

Sridhar M, Raoa R, Babaa NHK, Kumbharea RM (2007) Microwave-accelerated Gewald reaction Synthesis of 2-aminothiophenes. *Tetrahedron Lett* **48**:3171-3172

Suzuki M (2006) The Drosophila tweety family: molecular candidates for large-conductance Ca²⁺-activated Cl⁻ channels. *Exp Physiol* **91**, 141-147

Takahashi A, Sato Y, Shiomi Y, Cantarelli VV, Iida T, Lee M, and Honda T (2000) Mechanisms of chloride secretion induced by thermostable direct haemolysin of *Vibrio parahaemolyticus* in human colonic tissue and a human intestinal epithelial cell line. *J Med Microbiol* **49**:801-810

Tarran R, Loewen ME, Paradiso AM, Olsen JC, Gray MA, Argent BE, Boucher RC, and Gabriel SE (2002) Regulation of murine airway surface liquid volume by CFTR and Ca²⁺-activated Cl⁻ conductances. *J Gen Physiol* **120**:407-418

Thiagarajah JR, Verkman AS (2005) New drug targets for cholera therapy. *Trends Pharmacol Sci* **26**:172-175

Verkman AS (2004) Drug discovery in academia. *Am J Physiol* **286**:C465-C374.

MOL #43208

Verkman AS, and Jayaraman S (2002) Fluorescent indicator methods to assay functional CFTR expression in cells. *Methods Mol Med* **70**:187-196

Worrell RT and Frizzell RA (1991) CaMKII mediates stimulation of chloride conductance by calcium in T84 cells. *Am J Physiol* **260**:C877-C882

Yang H, Shelat AA, Guy RK, Gopinath VS, Ma T, Du K, Lukacs GL, Taddei A, Folli C, Pedemonte N, Galietta LV, and Verkman AS (2003) Nanomolar affinity small-molecule correctors of defective $\Delta F508$ -CFTR chloride channel gating. *J Biol Chem* **278**:35079-35085

Yangthara B, Mills A, Chatsudthiapong V, Tradtrantip L, and Verkman AS (2007) Small-molecule vasopressin-2 receptor antagonist identified by a G-protein coupled receptor 'pathway' screen. *Mol Pharmacol* **72**:86-94

MOL #43208

FOOTNOTES

* authors contributed equally

Supported by grants DK72517, HL73854, EB00415, EY13574, DK35124 and DK43840 from the National Institutes of Health, and Drug Discovery and Research Development Program grants from the Cystic Fibrosis Foundation.

MOL #43208

LEGENDS FOR FIGURES

Figure 1. Assay for CaCC inhibitor screening. (A) Principle of cell-based, fluorescence high-throughput screening assay. CaCC-facilitated iodide influx is measured from the kinetics of decreasing YFP-H148Q/I152L fluorescence in response to iodide addition to the extracellular solution. CaCC is activated by a mixture of calcium-elevating agonists. CCh, carbachol; m_3 AChR, carbachol receptor; P_{2Y2} , purinergic receptor; CaMKII, calcium-calmodulin protein kinase 2. (B) Fluorescence micrograph of lentivirus-infected HT-29 cells stably expressing the YFP iodide sensor.

Figure 2. Functional characterization of YFP-expressing HT-29 cells. Time course of YFP fluorescence after extracellular iodide addition. As indicated solutions contained histamine (100 μ M), calcimycin (10 μ M), ATP (100 μ M), carbachol (100 μ M), carbachol (100 μ M) + CFTR_{inh}-172 (20 μ M), or forskolin (20 μ M), individually (A), and in various combinations (at same concentrations) (B). The scale-bar on the y-axis indicates the percentage reduction in fluorescence relative to baseline fluorescence (before iodide addition). (C) Carbachol concentration-response study. (D) Initial negative fluorescence curve slope (following extracellular iodide addition) as a function of time after carbachol / ATP (each 100 μ M) addition and extracellular iodide addition.

Figure 3. CaCC inhibitor screening. (A) Screen validation. (left) Time course of YFP fluorescence in HT-29 cells following iodide addition in the absence or presence of carbachol (100 μ M) and ATP (100 μ M). (right) Histogram distribution of iodide influx rates ($d[I]/dt$) determined from initial fluorescence slopes. (B) (left) Examples of fluorescence data for individual compounds in the primary screen. (right) Histogram distribution of percentage inhibition from primary compound screening. Dashed vertical line denotes selection criteria for further evaluation.

MOL #43208

Figure 4. Structures and synthesis of putative CaCC inhibitors. (A) Structures of compounds of classes A-F identified from the primary screen. (B) Synthesis of CaCC_{inh}-A01: 6-t-butyl-2-(furan-2-carboxamido)-4,5,6,7-tetrahydrobenzo[b] thiophene-3-carboxylic acid, and CaCC_{inh}-B01: 2-hydroxy-4-(4-p-tolylthiazol-2-ylaminobenzoic acid. See Methods for details. (C) Concentration-inhibition data for CaCC_{inh}-A01 and CaCC_{inh}-B01 determined by plate reader fluorescence assay.

Figure 5. Target dissection studies. (A) Time course of YFP fluorescence in HT-29 cells following iodide addition in the absence or presence of thapsigargin in cells pre-treated with 30 μ M of indicated compounds. (B) YFP fluorescence in FRT cells expressing human wildtype CFTR following iodide addition in cells pre-treated with 30 μ M of indicated compounds. CFTR_{inh}-172 (20 μ M) was present where indicated. (C) Calcium signaling measured by fura-2 fluorescence in response to indicated agonists and test compounds. A, CaCC_{inh}-A01; B, CaCC_{inh}-B01. Representative data shown on the left, with averaged data on the right (SE, n = 3-4). Differences not significant. (D) ATP / carbachol-induced CaMKII phosphorylation determined by immunoblot analysis (representative of 3 separate experiments).

Figure 6. Patch-clamp analysis of CaCC inhibitors. CaCC channel activity in the whole-cell configuration was measured HT-29 cells. (A) Ionomycin-induced currents in asymmetrical solutions in the absence or presence of CaCC_{inh}-A01 or CaCC_{inh}-B01 (each 10 μ M) recorded at a holding potential at 0 mV, and pulsing to voltages between \pm 120 mV in steps of 20 mV (see Methods). (B) Current/voltage (I/V) plot of mean currents at the end of each voltage pulse from experiments as in A. (C) Summary of current density data measured at V_m of +100 mV (S.E., n = 6-8). (D) (top) Ionomycin-induced chloride currents in the whole-cell configuration with symmetrical NMDG-Cl solutions. (bottom) I/V plot of mean currents at the end of each voltage pulse.

MOL #43208

Figure 7. Inhibition of chloride secretion in T84 cells by short-circuit current analysis. (A)

After carbachol stimulation, ATP-induced I_{sc} was measured in the absence or presence of inhibitors (representative of 3-4 separate experiments). (B) Summary of short-circuit currents induced by carbachol and ATP for experiments as in A (S.E., n=3-4). (Inhibitors not present for carbachol stimulation). * $P < 0.05$ vs. control.

Figure 8. Structure-activity analysis of CaCC inhibitors. Summary of SAR conclusions for class A and B CaCC inhibitors. See text for explanations.

MOL #43208

TABLE 1 Structure-activity of Class A CaCC inhibitors

Compound	R1	R2	R3	n	% inhibition at 25 μ M
CaCC _{inh} -A01	t-butyl	OH	CO-furanyl	0	100
CaCC _{inh} -A02	t-butyl	OH	CO-2-methylphenyl	0	95
CaCC _{inh} -A03	t-butyl	OH	CO-3-chlorophenyl	0	50
CaCC _{inh} -A04	t-butyl	OH	CO-phenyl	0	85
CaCC _{inh} -A05	t-butyl	OH	CO-2-chlorophenyl	0	75
CaCC _{inh} -A06	t-butyl	OEt	CO-CH ₂ CH ₂ CO ₂ H	0	75
CaCC _{inh} -A07	t-butyl	OEt	(trans)COCH=CHCO ₂ H	0	98
CaCC _{inh} -A08	t-butyl	OEt	CO-2-carboxycyclohexyl	0	80
CaCC _{inh} -A09	t-butyl	OMe	CO-CH ₂ CH ₂ CH ₂ CO ₂ H	0	45
CaCC _{inh} -A10	EtMe ₂ C-	OEt	CO-2-carboxycyclohexyl	0	75
CaCC _{inh} -A11	t-butyl	OMe	CO-CH ₂ CH ₂ CO ₂ H	0	81
CaCC _{inh} -A12	H	OH	CO-4-methylphenyl	1	15
CaCC _{inh} -A13	H	OH	CO-phenyl	1	27
CaCC _{inh} -A14	H	OH	CO-2-chlorophenyl	1	18
CaCC _{inh} -A15	H	OH	CO-3-methoxyphenyl	0	20
CaCC _{inh} -A16	t-butyl	NH-3-MePh	CO-CH ₂ CH ₂ CO ₂ H	0	42
CaCC _{inh} -A17	H	OH	CO-3-methylphenyl	0	07
CaCC _{inh} -A18	t-butyl	NH-4-MeOPh	CO-CH ₂ CH ₂ CO ₂ H	0	35

See Fig. 8 for locations of R1, R2 and R3, and meaning of n. Ph = phenyl, Br = bromo, Cl = chloro, F = fluoro, OMe = methoxy, NO₂ = nitro

MOL #43208

TABLE 2. Structure-activity of Class B CaCC inhibitors

Compound	R1	R2	R3	% inhibition at 25 μ M
CaCC _{inh} -B01	4-Me	-H	3-Carboxylate-4-hydroxyphenyl	100
CaCC _{inh} -B02	4-Me	-CH ₂ CO ₂ H	3-Chloro-4-methylphenyl	40
CaCC _{inh} -B03	4-Me	-CH ₂ CO ₂ H	3-Bromophenyl	60
CaCC _{inh} -B04	4-Me	-CH ₂ CO ₂ H	2,4-Dichlorophenyl	65
CaCC _{inh} -B05	4-Me	-CH ₂ CO ₂ H	3-Trifluoromethylphenyl	60
CaCC _{inh} -B06	2,4-DiMe	-Pr	4-Carboxylatephenyl	100
CaCC _{inh} -B07	2,4-DiMe	-CH ₂ CO ₂ H	4-Bromophenyl	70
CaCC _{inh} -B08	2,4-DiMe	-CH ₂ CO ₂ H	3-Trifluoromethylphenyl	75
CaCC _{inh} -B09	4-PhO	-H	4-Isobutylphenyl	65
CaCC _{inh} -B10	3-CF ₃	-H	4-Cyclohexylphenyl	55
CaCC _{inh} -B11	4-Me	-CH ₂ CO ₂ H	4-Ethoxyphenyl	65
CaCC _{inh} -B12	4-Me	-Ph	CO-3-Methylphenyl	3
CaCC _{inh} -B13	4-Me	-H	Ethyl	20
CaCC _{inh} -B14	4-MeO	-CH ₂ CH ₂ CO ₂ H	4-Methoxyphenyl	18

See Fig. 8 for locations of R1, R2 and R3, and meaning of n. Ph = phenyl, Br = bromo, Cl = chloro, F = fluoro, OMe = methoxy, NO₂ = nitro

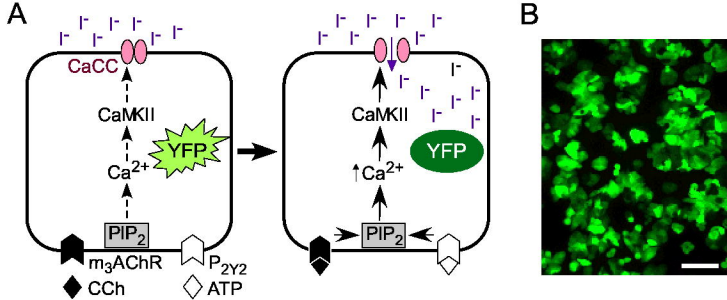


Figure 1

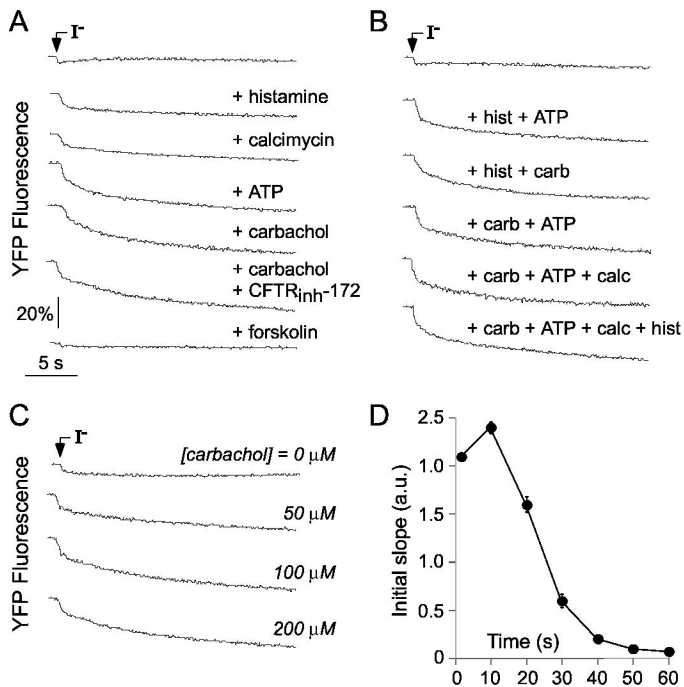


Figure 2

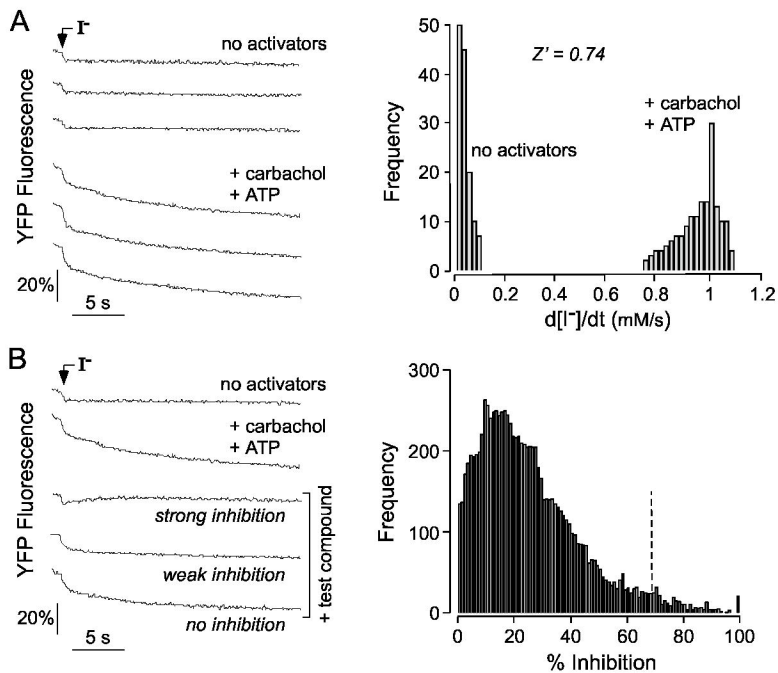


Figure 3

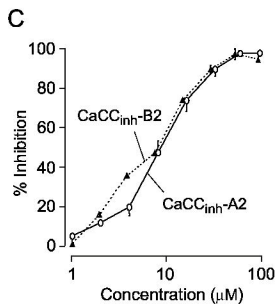
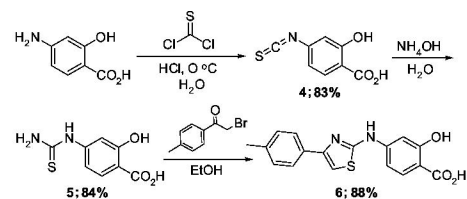
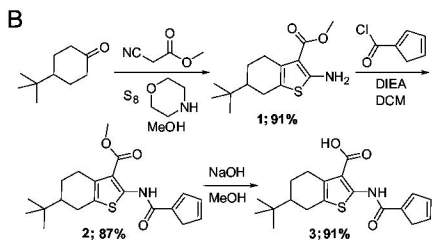
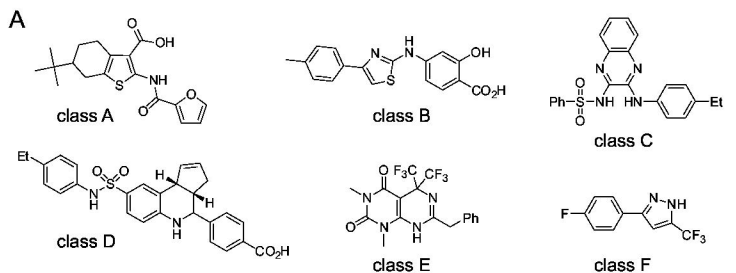


Figure 4

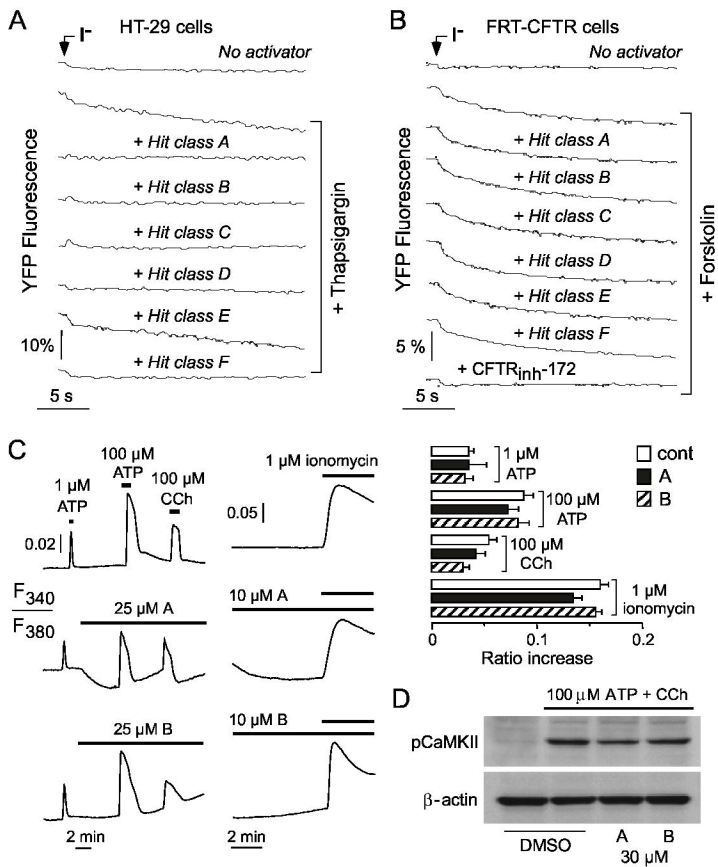


Figure 5

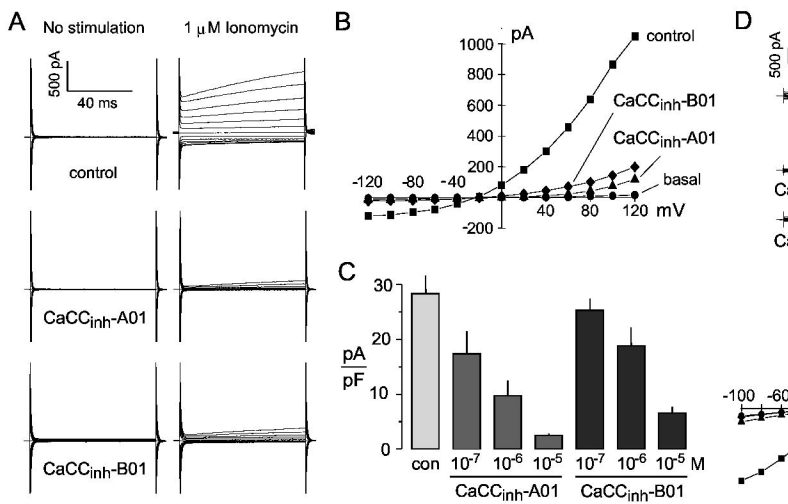


Figure 6

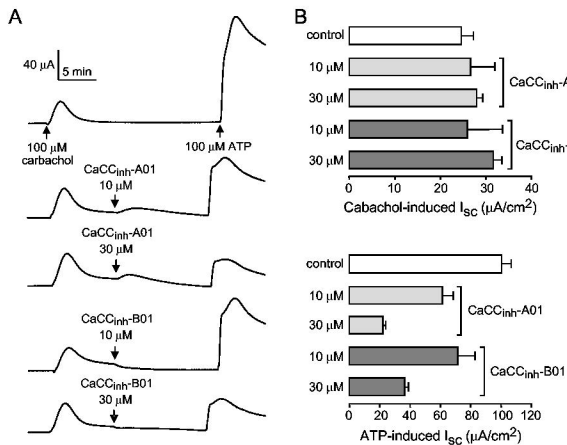
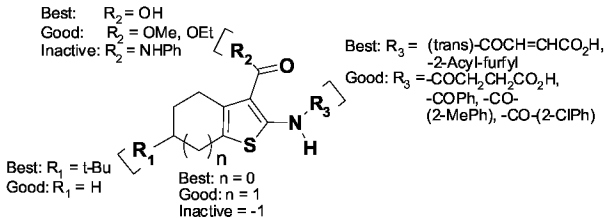
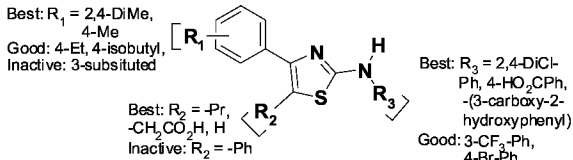


Figure 7



Class A



Class B

Figure 8